Essential function of α-calcium/calmodulin-dependent protein kinase II in neurotransmitter release at a glutamatergic central synapse

Heather L. Hinds*†, Ivan Goussakov†‡, Kazu Nakazawa*, Susumu Tonegawa*, and Vadim Y. Bolshakov‡§

*Howard Hughes Medical Institute, Picower Center for Learning and Memory, RIKEN-MIT Neuroscience Research Center, Departments of Biology and Brain and Cognitive Sciences, Massachusetts Institute of Technology, Cambridge, MA 02139; and ‡McLean Hospital, Department of Psychiatry, Harvard Medical School, 115 Mill Street, Belmont, MA 02478

A significant fraction of the total calcium/calmodulin-dependent protein kinase II (CaMKII) activity in neurons is associated with synaptic connections and is present in nerve terminals, thus suggesting a role for CaMKII in neurotransmitter release. To determine whether CaMKII regulates neurotransmitter release, we generated and analyzed knockout mice in which the dominant α-isoform of CaMKII was specifically deleted from the presynaptic side of the CA3-CA1 hippocampal synapse. Conditional CA3 α-CaMKII knockout mice exhibited an unchanged basal probability of neurotransmitter release at CA3-CA1 synapses but showed a significant enhancement in the activity-dependent increase in probability of release during repetitive presynaptic stimulation, as was shown with the analysis of unitary synaptic currents. These data indicate that α-CaMKII serves as a negative activity-dependent regulator of neurotransmitter release at hippocampal synapses and maintains synapses in an optimal range of release probabilities necessary for normal synaptic operation.

Synapses mediate interneuronal communication and display a variety of properties (1). Presynaptic neurotransmitter release is one of the first steps in the sequence of events underlying synaptic transmission. Discrete packets of neurotransmitter encased in vesicles are released at synaptic connections with a certain probability (probability of release, P_r) in a tightly regulated fashion (1, 2). Calcium/calmodulin-dependent protein kinase II (CaMKII), a serine/threonine protein kinase, is well positioned to serve a role in synaptic function regulation, because it is highly expressed in the brain and is known to phosphorylate multiple synaptic proteins (2). Accordingly, CaMKII has previously been implicated in the long-lasting frequency-dependent regulation of synaptic function in mammals (3–9), birds (10), frogs (11), and invertebrates (12).

Although a postsynaptic role for CaMKII in synaptic function and plasticity has been well demonstrated (3, 4, 6, 7, 13), studies of the presynaptic function of this enzyme are scarce. Early microinjection experiments in the squid giant synapse showed that CaMKII injected presynaptically enhanced neurotransmitter release (14, 15). This effect appeared to be mediated by phosphorylation of a synaptic vesicle protein, synapsin I, which in its dephosphorylated form inhibited synaptic transmission. However, mice lacking synapsin I do not demonstrate a major change in the basal P_r (16), suggesting that certain differences in the mechanisms of release may exist between vertebrate and invertebrate synapses. It has also been shown that α-CaMKII can either potentiate or depress CA3-CA1 synapses in the hippocampus depending on the pattern of presynaptic activation. Paired-pulse facilitation (PPF), an index of presynaptic function, was decreased in the CA1 region of mice heterozygous for a global null mutation of α-CaMKII, whereas another form of presynaptic plasticity, which also depends on P_r, posttetanic potentiation, was enhanced (17). A direct estimate of P_r was not previously obtained in global CaMKII knockout (KO) mice, either under resting conditions or during repetitive presynaptic

activation. Thus, the specific function of CaMKII in presynaptic mechanisms at mammalian central synapses, which may play a role in synaptic plasticity, is largely unknown.

In this study, we tested the hypothesis that CaMKII in presynaptic nerve terminals is involved in the regulation of neurotransmitter release by creating and analyzing a new strain of mice in which CaMKII gene deletion is restricted to adult CA3 hippocampal pyramidal cells. This allowed us to ask the question of how CaMKII contributes to synaptic transmission specifically on the presynaptic side of the important CA3-CA1 mammalian synapse. Using these highly specific α-CaMKII deficient mice, we found that despite unchanged basal probability of neurotransmitter release, the mutant synapses exhibit a significant enhancement of synaptic responses during repetitive presynaptic stimulation. We further showed with the analysis of unitary synaptic responses that this effect is associated with an increased probability of neurotransmitter release. Our study provides support to the notion that α-CaMKII serves an essential function in neurotransmitter release during repetitive presynaptic activity by maintaining synapses in an optimal range of release probabilities necessary for normal synaptic operation.

Materials and Methods

Generation of CA3 α-CaMKII KO Mice. A more detailed description of experimental procedures is available in the supporting information on the PNAS web site, www.pnas.org. A mouse C57BL/6 bacterial artificial chromosome (BAC) library (Genome Systems, St. Louis) was screened by using an *Eco*R1-*Xma*I 440-bp fragment from the 5′ end of the α-CaMKII cDNA. A BAC was isolated that contained the 5′ end of the α-CaMKII genomic locus, including the targeted exon 2 (18) and was used to prepare the targeting construct. One loxP site was inserted into intron 1 and a LFNT cassette [a pair of *lox*P sites, a pair of FLP recombinase target (FRT) sites, and neomycin (neo) and thymidine kinase (tk) selection markers] was inserted into intron 2, as shown in Fig. 1. The diphtheria toxin gene was placed at the 3′ end of the construct to select against nonhomologous recombinants. Fifty micrograms of the linearized targeting vector was transfected into C57BL/6 ES cells by electroporation, cells were grown under G418 selection, and resistant colonies were screened for homologous recombination by using 5′ and 3′ external probes. Successful recombinants were expanded and transfected again by electroporation with 50 μg of FLPe (19). After gangcyclover selection, resistant colonies were screened for removal of the neo-tk ($f\alpha$-CaMKII allele) by using external and internal probes. $f\alpha$-CaMKII ES cell clones were injected into blastocysts (BALB/c background) and recombinant "floxed"

NEUROSCIENCE

Fig. 1. Generation of $f\alpha$-CaMKII recombinant mice. (*a Top*) Region of the wild-type α-CaMKII locus containing the targeted exon 2. (*Middle*) α-CaMKII targeting vector with a loxP site inserted into intron 1 and an LFNT cassette containing neo-tk and recombinase recognition sites inserted into intron 2. (*Bottom*) $f\alpha$-CaMKII locus. Cre/loxP mediated recombination at the $f\alpha$-CaMKII locus will excise 4 kb of sequence that includes exon 2. Open triangle, loxP; open oval, FRT; neo, neomycin resistance gene; tk, thymidine kinase gene; DT-A, diphtheria toxin gene. Restriction enzymes: B, *Bam*HI; R1, *Eco*RI; Sp, *Spe*I; N, *Nco*I; X, *Xho*I; Sm, *Sma*I. (*b*) Tail DNA digested with *Bam*HI and screened with a 3′ probe external to the recombined locus. +/+, wild type; +/f, heterozygous; f/f, homozygous $f\alpha$-CaMKII.
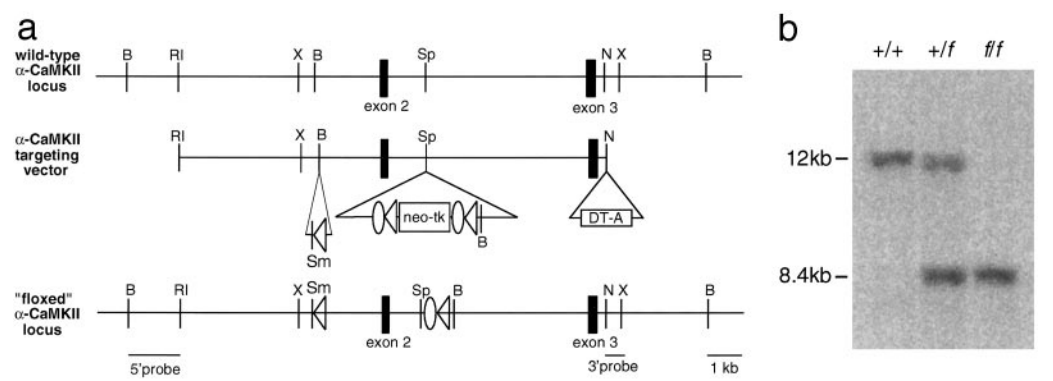
$f\alpha$-CaMKII mice were produced, as previously described (20). $f\alpha$-CaMKII mice were crossed with G32-4 Cre recombinase transgenic mice (21) to produce ($f\alpha$-CaMKII/$f\alpha$-CaMKII, Cre/+) conditional KO mice (CA3 α-CaMKII KO).

In Situ Hybridization. Fresh frozen sections (14 μm) of mouse brains were fixed with 4% paraformaldehyde (PFA) and hydridized with a ^{33}P-labeled 46-bp oligonucleotide cRNA probe (Riboprobe System Kit, Promega) specific for exon 2 of α-CaMKII or or β-CaMKII. Hybridized sections were washed, dipped in Kodak NTB3 nuclear emulsion, and exposed for 2 weeks at 4°C. Dark-field images were captured and digitized by using a Spot charge-coupled device camera and software system (Diagnostic Instruments, Sterling Heights, MI), with mRNA signal shown by white grains.

Immunohistochemistry. Mice were perfused transcardially with 4% paraformaldehyde (PFA) and brains were removed and postfixed overnight at 4°C. Fifty-micrometer-thick sagittal Vibratome sections were cut and labeled with an anti-α-CaMKII primary monoclonal antibody (1:500, Boehringer/Chemicon) followed by a biotinylated horse anti-mouse IgG (1:200, Vector) secondary antibody. Immunoreactivity was visualized by streptavidin–biotin/horseradish peroxidase complex (Vector) formation and amplification with FITC-tyramide (NEN). Fluorescent images were captured by using a confocal laser scanning microscope (Bio-Rad).

Electrophysiological Analysis. Electrophysiology experiments were performed on male mice between the ages of 4–5.5 mo. $f\alpha$-CaMKII littermates were used as controls, and all experiments were performed blind to genotype. Hippocampal slices (250–300 μm) were superfused in solution containing (in mM) 119 NaCl, 2.5 KCl, 2.5 CaCl$_2$, 1.0 MgSO$_4$, 1.25 NaH$_2$PO$_4$, 26.0 NaHCO$_3$, 10 glucose, and 0.1 picrotoxin and equilibrated with 95% O$_2$ and 5% CO$_2$ (pH 7.3–7.4) at room temperature. Whole-cell recordings of excitatory postsynaptic currents (EPSCs) were obtained from CA1 pyramidal cells under visual guidance (differential interference contrast microscopy /infrared optics) with an EPC-9 amplifier and PULSE Ver. 8.09 software (HEKA Electronics, Lambrecht/Pfalz, Germany). The patch electrodes (3–5 MΩ resistance) contained 120 mM K-gluconate, 5 mM NaCl, 1 mM MgCl$_2$, 0.2 mM EGTA, 10 mM Hepes, 2 mM MgATP, and 0.1 mM NaGTP (adjusted to pH 7.2 with KOH). To examine the frequency dependence of the EPSCs, 10 mM calcium chelator EGTA was used to prevent long-term potentiation. Series resistance was monitored throughout the experiment and was in the range of 10–20 MΩ. Currents were filtered at 1 kHz and digitized at 5 kHz. The holding potential was -70 mV. In all experiments, the stimulus intensity was adjusted to produce synaptic responses with a relatively similar baseline ESPC amplitude in both control and KO mice. Unitary EPSCs were evoked by

low-intensity current pulses (25–100 μA; 100-μs duration) applied through a fine-tipped ($\approx$2 μM) concentric stimulating electrode consisting of a patch pipette that was coated with silver paint (22). To calculate failure rates, a method of visual classification of failures was used (23). The spontaneous miniature EPSCs were recorded on videotape for offline analysis in the presence of 1 μM tetrodotoxin.

Results

CA3 α-CaMKII KO Mice. We generated conditional α-CaMKII KO mice by using the bacteriophage P1-derived Cre/loxP recombination system (24) in which the dominant α-isoform of CaMKII was deleted specifically in hippocampal CA3 pyramidal cells. First, a C57BL/6 murine genomic clone was isolated that contained the 5′ end of the α-CaMKII genomic locus, including the putative ATP-binding site in exon 2 (ref. 18; also see supporting information on the PNAS web site). This was used to prepare a targeting vector for homologous recombination that consisted of genomic sequence flanking exon 2, strategically placed positive (neomycin resistance), and negative (thymidine kinase, diphtheria toxin) selectable markers, and appropriate recombinase target sites (Fig. 1). After homologous recombination in C57BL/6 embryonic stem (ES) cells (25) and removal of the neo-tk selection cassette by transfection of ES cells with FLPe recombinase (19), ES clones were injected into BALB/c blastocysts to produce "floxed" α-CaMKII mice ($f\alpha$-CaMKII). To obtain selective deletion of exon 2 in the CA3 region of the hippocampus, $f\alpha$-CaMKII mice were crossed to a transgenic line (G32-4) expressing Cre recombinase driven by the kainate receptor KA-1 promoter. This Cre transgenic line has been previously shown to give selective gene knockout in hippocampal CA3 pyramidal cells when crossed to N-methyl-D-aspartate (NMDA) receptor subunit 1 (NR1) "floxed" mice (21). Crosses between $f\alpha$-CaMKII and G32-4 Cre mice were performed to obtain ($f\alpha$-CaMKII/$f\alpha$-CaMKII, Cre/+) mutant mice (CA3 α-CaMKII KO) and homozygous "floxed" ($f\alpha$-CaMKII/$f\alpha$-CaMKII, +/+) littermate controls ($f\alpha$-CaMKII), which were the focus of our analyses.

In situ hybridization studies with an oligonucleotide probe specific for the floxed exon 2 demonstrated restricted deletion of $f\alpha$-CaMKII exon 2 in the CA3 region of the hippocampus in CA3 α-CaMKII KO mice (Fig. 2 a–d). Deletion was first detected in CA3 pyramidal cells at 1 mo, increasing with age and reaching a plateau of 90–95% gene knockout in 3-mo-old CA3 α-CaMKII KO mice (Fig. 2 e–h). A very small amount (less than a few percent) of deletion was observed in dentate granule cells in 4-mo-old animals, but absolutely no deletion was seen in the pyramidal cells of the CA1 region of the hippocampus, or in other brain regions, at all ages. Consequently, we have produced a specific knockout of α-CaMKII only in presynaptic cells at the CA3 Schaffer collateral–CA1 synapses. *In situ* hybridization studies of homozygous floxed
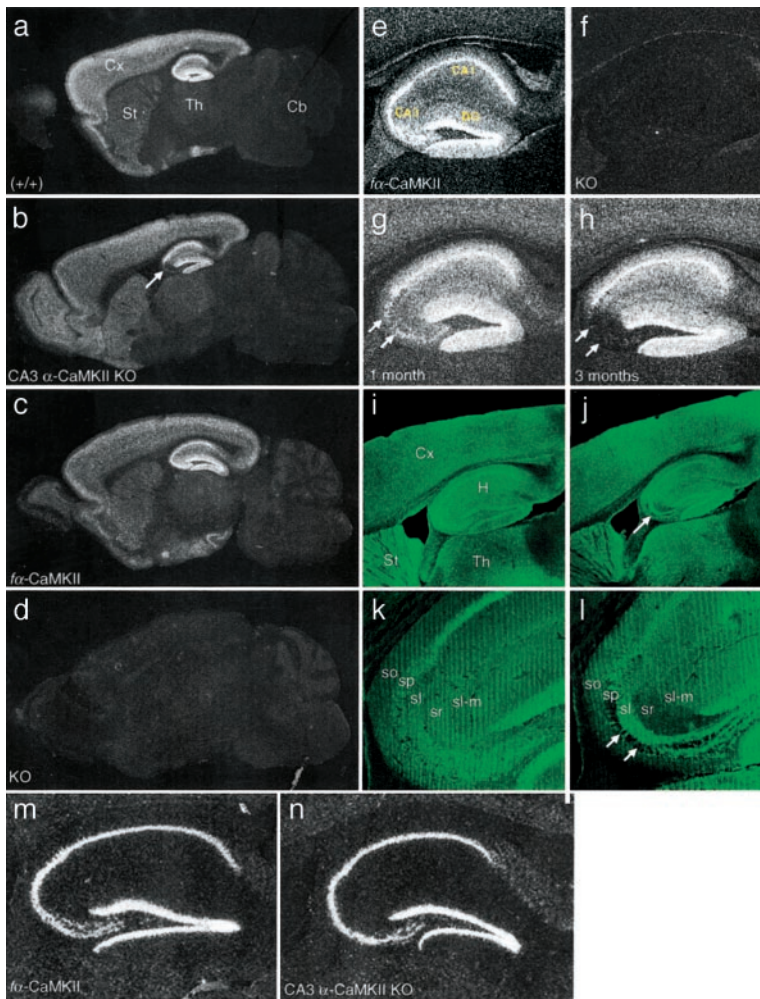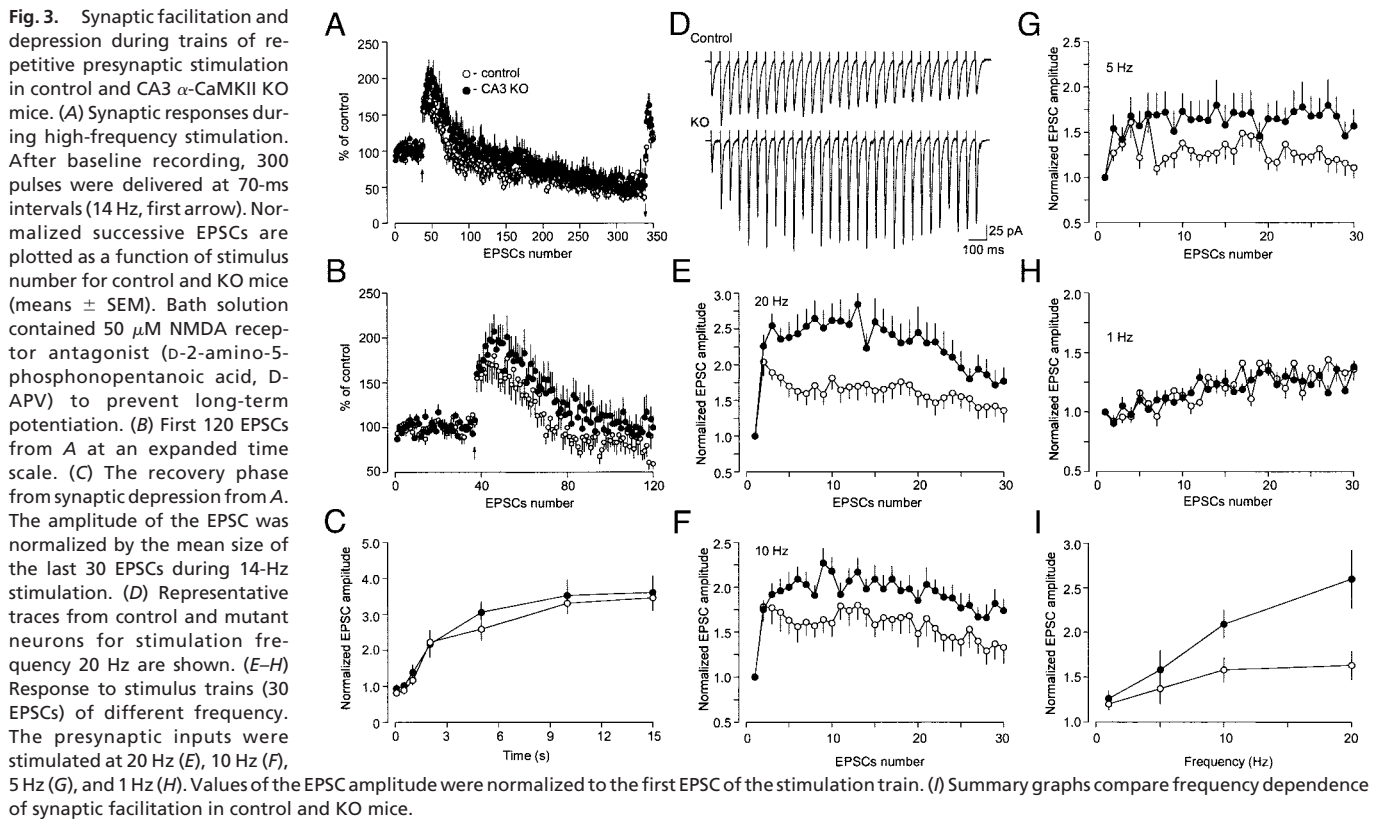
Fig. 2. Expression studies of CA3 α-CaMKII KO mice. (*a*–*d*) Dark field images of sagittal brain sections from 4-mo-old wild-type (*a*), α-CaMKII floxed (*c*), CA3 α-CaMKII KO (*b*), and global α-CaMKII KO (*d*) mice hybridized with an α-CaMKII-specific probe. Deletion of the $f\alpha$-CaMKII gene was specific to hippocampal CA3. Cx, cortex; St, striatum; Th, thalamus; Cb, cerebellum. Arrow in *b* indicates the location of hippocampal CA3. (*e*–*h*) Dark-field higher magnification images of the hippocampus from α-CaMKII floxed (*e*), global α-CaMKII KO (*f*), and 1- (*g*) and 3-mo-old (*h*) CA3 α-CaMKII KO mice after hybridization with a probe specific for α-CaMKII. These images show that gene knockout is highly specific to the CA3 region of the hippocampus, indicated with double arrows. DG, dentate gyrus. (*i*–*l*) Confocal images from 3-mo-old floxed (*i* and *k*) and 4-mo-old CA3 α-CaMKII KO (*j* and *l*) mice after immunochemical staining with anti-α-CaMKII antibody. Lower-magnification sagittal images on top, followed by high-magnification images of hippocampal CA3 show that the α-CaMKII protein is absent from the vast majority of pyramidal cell bodies (stratum pyramidale; indicated with arrows) and dendrites (strata radiatum, oriens) in the CA3 region, whereas axons projecting from dentate granule cells to the stratum lucidum are strongly stained. H, hippocampus; sp, stratum pyramidale; sr, stratum radiatum; so, stratum oriens; sl, stratum lucidum; sl-m., stratum lacunosum-moleculare; GL, granule layer; ML, molecular layer. (*m* and *n*) Dark-field images of the hippocampus from 4-mo-old floxed (*m*) and CA3 α-CaMKII KO mice (*n*) after hybridization with a probe specific for β-CaMKII. No compensatory increase in β-CaMKII expression was observed in hippocampal regions.

($f\alpha$-CaMKII/$f\alpha$-CaMKII, +/+) mice demonstrated that the insertion of loxP sequences alone did not affect normal expression from the α-CaMKII locus (Fig. 2 *c* and *e*), and consequently, these animals were used as controls ($f\alpha$-CaMKII) in subsequent experiments.

Immunohistochemistry using an α-CaMKII monoclonal antibody on fixed vibratome sections revealed staining patterns consistent with *in situ* hybridization studies; α-CaMKII protein was clearly absent in regions where recombination had occurred (Fig. 2 *i*–*l*). α-CaMKII protein was visible in only 5–10% of CA3 pyramidal cells in 4-mo-old CA3 α-CaMKII KO mice. We saw a dramatic reduction in staining specifically in the CA3 cell body layer (stratum pyramidale) and in CA3 dendritic layers (stratum radiatum, stratum oriens), whereas dentate gyrus granule cell axons projecting to the CA3 stratum lucidum layer were highly stained for α-CaMKII protein (Fig. 2 *j* and *l*). CA3 Schaffer collateral axons travel to the CA1 stratum radiatum and oriens and form synapses on CA1 dendrites, and we observed a decrease in CA3 axonal staining in a high background of CA1 dendritic α-CaMKII protein in these areas (Fig. 2*j*). No CA1 pyramidal cells showed a loss of α-CaMKII protein, confirming that we have produced a conditional gene deletion of α-CaMKII that is both spatially and temporally specific, allowing us to avoid widespread deficits due to global deletion or abnormal early development. Neither immunohistochemical nor *in situ* hybridization studies revealed any gross anatomical abnormalities in CA3 α-CaMKII KO mice (Figs. 1 and 2), and CA3 pyramidal cells have normal morphology and cell density in these mutants (see supporting information on the PNAS web site).

CA3 α-CaMKII KO mice appeared quite normal in general behavior, with no obvious sign of sensory or motor impairments and normal viability and fertility (data not shown). Although the α isoform of CaMKII is the dominant isoform expressed in the brain, the lesser β isoform is also expressed in the hippocampus (6). It is possible that up-regulation of β-CaMKII could occur to compensate for the absence of the α isoform in CA3 α-CaMKII KO mice. However, *in situ* hybridization in mutant and control mice using a probe specific for β-CaMKII did not reveal changes in expression pattern (Fig. 2 *m* and *n*), indicating that such compensation has not occurred.

Rate of Depletion of Vesicles Available for Release. By analyzing these highly specific CaMKII-deficient mice, we are now able to ask how CaMKII contributes to synaptic function specifically at the presynaptic side of the CA3-CA1 synapse, a question that has been limited previously by technical difficulties in delivering specific inhibitors directly to presynaptic sites in mammalian systems. To explore the role of CaMKII in presynaptic function, we stimulated CA3 Schaffer collateral/commisural fibers and recorded EPSCs in CA1 pyramidal neurons in hippocampal slices from CA3 α-CaMKII KO mice and $f\alpha$-CaMKII littermate controls. EPSCs of grossly normal size and shape were observed in KO mice, suggesting that the basic neurotransmitter release machinery is functional in the absence of α-CaMKII in presynaptic CA3 cells (Figs. 3 and 4 *A* and *B*). Because the size of the releasable vesicle pool may determine Pr (26), we then investigated whether the deletion of α-CaMKII in presynaptic CA3 neurons affects the size of the pool. We measured the rate of

Fig. 3. Synaptic facilitation and depression during trains of repetitive presynaptic stimulation in control and CA3 α-CaMKII KO mice. (*A*) Synaptic responses during high-frequency stimulation. After baseline recording, 300 pulses were delivered at 70-ms intervals (14 Hz, first arrow). Normalized successive EPSCs are plotted as a function of stimulus number for control and KO mice (means ± SEM). Bath solution contained 50 μM NMDA receptor antagonist (D-2-amino-5-phosphonopentanoic acid, D-APV) to prevent long-term potentiation. (*B*) First 120 EPSCs from *A* at an expanded time scale. (*C*) The recovery phase from synaptic depression from *A*. The amplitude of the EPSC was normalized by the mean size of the last 30 EPSCs during 14-Hz stimulation. (*D*) Representative traces from control and mutant neurons for stimulation frequency 20 Hz are shown. (*E–H*) Response to stimulus trains (30 EPSCs) of different frequency. The presynaptic inputs were stimulated at 20 Hz (*E*), 10 Hz (*F*), 5 Hz (*G*), and 1 Hz (*H*). Values of the EPSC amplitude were normalized to the first EPSC of the stimulation train. (*I*) Summary graphs compare frequency dependence of synaptic facilitation in control and KO mice.

depletion of vesicles available for release in control and CA3 α-CaMKII KO mice in response to long trains of high-frequency presynaptic stimulation (300 pulses at 70-ms interstimulus interval). Depletion of the readily releasable pool of synaptic vesicles, although acting in parallel with transient inactivation of release sites after the release event occurred (refractory depression, refs. 27 and 28), dominates synaptic depression during long periods of presynaptic stimulation (28). Therefore, the rundown of synaptic responses observed under our stimulation conditions reflects depletion of the releasable pool. Testing the notion that the size of the pool could be different in control and CA3 α-CaMKII KO mice, we found that the extent of synaptic depression in response to repetitive stimulation of synapses was virtually identical in control (13 cells/10 mice) and CA3 α-CaMKII KO (17 cells/8 mice) groups (Fig. 3*A*; average of last 20 EPSCs in a train was used for the comparison; *t* test; *t* = 0.88, *P* = 0.4). The recovery rate from synaptic depression, which is a form of Ca^{2+}-dependent synaptic plasticity (29, 30), was also unaffected in CA3 α-CaMKII KO mice (Fig. 3*C*; no significant difference, *P* = 0.56, F[1,27] = 0.34, two-way ANOVA), suggesting that α-CaMKII is not essential for vesicular cycling in general, including control of the size of the releasable vesicle pool.

Frequency Facilitation. Although synaptic depression was not affected in CA3 α-CaMKII KO mice, the initial facilitation of the EPSC amplitude during repetitive stimulation of synaptic inputs (frequency facilitation), which depends primarily on an increase in *P*r (30), was significantly enhanced (Fig. 3 *A* and *B*). To explore this in more detail, we examined the magnitude of frequency facilitation in control (12 cells/5 mice) and KO (12 cells/5 mice) animals using different frequencies of stimulation and found that the CA3 α-CaMKII-deficient synapses display significantly enhanced facilitation of the EPSC amplitude at stimulation frequencies higher than 10 Hz (Fig. 3 *D–I*). For all of the frequencies tested (1–20 Hz), facilitation of the CA3-CA1 EPSC amplitude reached a plateau level by about the 15th stimulus. Therefore, we used the mean value

of the normalized EPSC amplitude reached by stimulus 15 in a train to compare the magnitude of frequency facilitation between the two experimental groups (Fig. 3*I*; significant difference, *P* < 0.03, F[1,21] = 5.84, two-way ANOVA).

Basal *Pr* Estimates. The enhanced frequency facilitation observed in CA3 α-CaMKII KO mice suggested that *P*r might be lower at mutant synapses, because this form of synaptic plasticity displays inverse dependence on the basal *P*r. Thus we asked whether presynaptically located α-CaMKII is involved in regulation of *P*r at the CA3-CA1 hippocampal synapses. To address this question, we measured paired pulse facilitation (PPF), an enhanced response to a second of two closely spaced presynaptic stimuli (30), in both control and CA3 α-CaMKII-deficient synapses at several interpulse intervals (50–300 ms). PPF is considered to be a mostly presynaptic phenomenon that, similar to frequency facilitation, depends on *P*r. Despite the fact that frequency facilitation was significantly altered in mutant mice, PPF was not affected in mutant (14 cells/5 mice) as compared with control (14 cells/5 mice) synapses (Fig. 4 *B* and *C*, no significant difference, *P* = 0.26, F[1,26] = 1.3, two-way ANOVA), suggesting that *P*r was not changed as a result of CA3 α-CaMKII deletion. Consistent with this, we also found no differences in synaptic input–output curves, which provide an integral measure of synaptic strength (Fig. 4*A*; data from 17 slices/6 control mice, and from 14 slices/5 KO mice; no significant difference, *P* = 0.89, F[1,29] = 0.02, two-way ANOVA). The frequency of spontaneous miniature EPSCs, another index of presynaptic function, was unaffected by CA3 α-CaMKII deletion (0.6 ± 0.1 Hz in 6 cells/4 control mice, and 0.7 ± 0.2 Hz in 4 cells/3 KO mice; no significant difference, *t* test, *t* = 0.45, *P* = 0.67).

The values of *P*r in different synaptic inputs to the same CA1 neuron are continuously distributed, suggesting that an infinite (continuous) number of *P*r values can exist in the population of inputs to a given postsynaptic cell (31). PPF measurements may not be sufficiently sensitive to show differences between population of

Hinds *et al.*
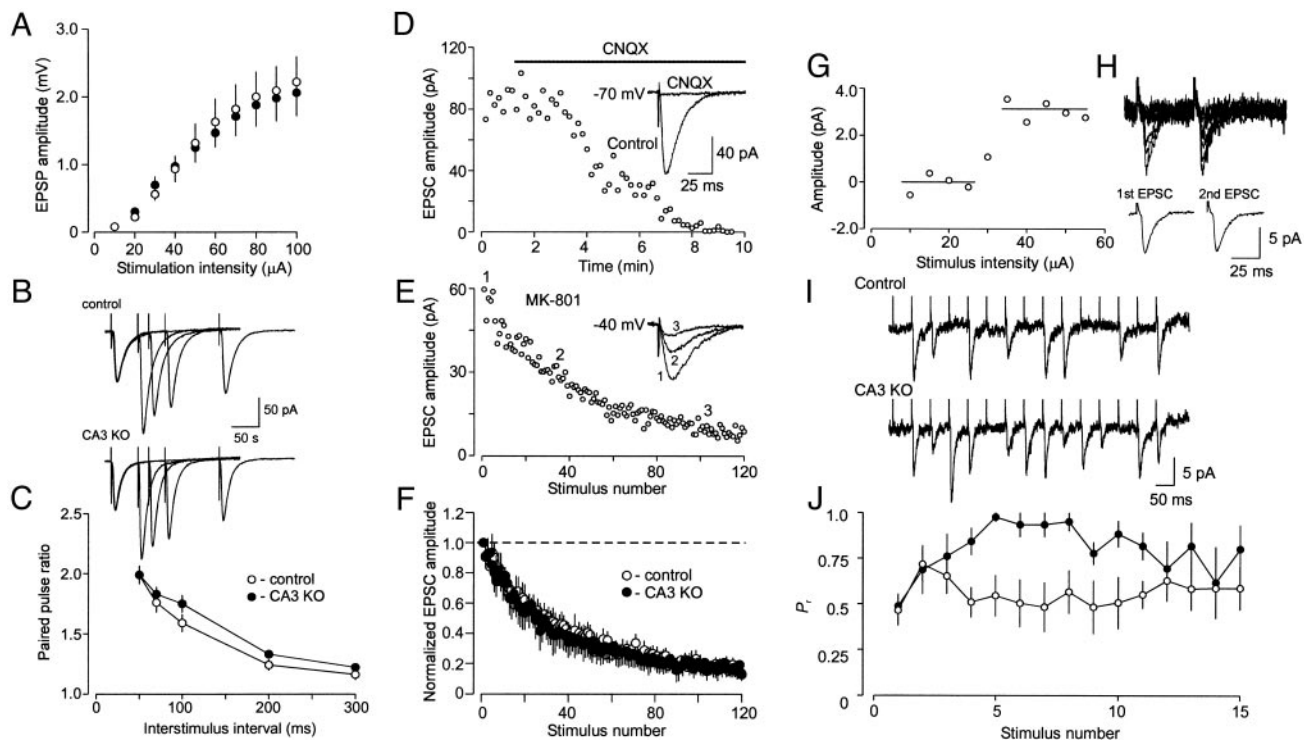
Fig. 4. Synaptic release probability at hippocampal CA3-CA1 synapses in control and CA3 α-CaMKII KO mice. (*A*) Comparison of synaptic efficacy using synaptic input–output curves. The extracellular field potential amplitude is plotted as a function of stimulation intensity. (*B*) Examples (average of 10 EPSCs) of PPF in control (*Upper*) and mutant (*Lower*) synapses. (*C*) PPF is plotted as a function of the interstimulus interval. Pairs of EPSCs were elicited 10–15 times for each interval tested. The values of PPF were calculated and averaged for each interstimulus interval. To calculate PPF, the EPSC for the second pulse was normalized to the EPSC induced by the first pulse. (*D–F*) Rate of MK-801 blockade is not altered in KO mice. (*D*) Synaptic responses were blocked by bath application of 20 μM 6-cyano-7-nitroquinoxaline-2,3-dione at a holding potential of −70 mV. (*E*) The progressive block by MK-801 (40 μM) of the NMDA receptor EPSC recorded from the same cell as in *D* at a holding potential of −40 mV. MK-801 was applied to the slice in the absence of presynaptic stimulation for 10 min. To measure rate of MK-801 block, the Schaffer collateral input was stimulated at 0.1 Hz frequency. EPSC amplitudes were normalized by the first EPSC. (*F*) Averaged data from control (open circles) and KO (filled circles) mice. Error bars show SEM. (*G*) An example of the intensity threshold test in a slice from control mouse. Mean EPSCs are shown as a function of stimulation current intensity (20 individual responses were averaged to obtain each point). Note the sharp threshold for the appearance of the EPSC, which indicates stimulation of a single presynaptic input. (*H*) Superimposed successive CA1 EPSCs recorded in response to minimal paired stimulation (50-ms interval, *Upper*) of a single CA3 neuron. (*Lower*) Traces represent average of successes only (potency) for first (*Left*) and second (*Right*) EPSCs. Potency value for first EPSC = 6.3 pA; for second EPSC, =6.2 pA. (*I*) Representative traces of unitary EPSCs recorded in response to short trains (15 stimuli, 50-ms interpulse interval) of presynaptic stimulation in slices from control (*Upper*) and CA3 α-CaMKII KO (*Lower*) mice. (*J*) Estimates of release probability at unitary synapses during repetitive stimulation in slices from control (open circles) and KO (filled circles) mice. Trains of unitary EPSCs were elicited 8–12 times for each cell tested. All unitary responses were classified as 1 (successes) or 0 (failures of synaptic transmission). The obtained parameters were then averaged for each individual experiment to provide an estimate of probability of success (the situation when release occurred).

synapses when the initial *P*r at a fraction of the activated synapses is very low (22). If the CaMKII mutation has differential effects on synapses with different initial *P*r, preferentially affecting low *P*r synapses, then an independent approach allowing us to estimate differences in the all-inclusive distribution of release probabilities at the CA3-CA1 hippocampal synapses is required. We therefore measured the rate of blockade of the NMDA receptor-mediated whole-cell EPSC by MK-801, an irreversible open-channel blocker of the NMDA receptors. Because MK-801 blocks NMDA receptor channels only when they are open, the rate of decline of the NMDA receptor-mediated EPSC in the course of repetitive presynaptic stimulation in the presence of MK-801 is determined by *P*r (32, 33). Accordingly, there should be a change in rate of MK-801 blockade associated with a change in release probability. We measured the rate of the progressive block of the NMDA receptor EPSC by MK-801 in the presence of 6-cyano-7-nitroquinoxaline-2,3-dione (20 μM), to block α-amino-3-hydroxy-5-methyl-4-isoxazolepropionic acid receptors, at a holding potential of −40 mV under whole-cell voltage–clamp conditions. The Mg^{2+} block of the NMDA receptor is relieved at this holding potential, allowing NMDA receptors to function. When MK-801 blocking rates were measured in slices from control and CA3 α-CaMKII KO mice,

there was no difference between both experimental groups (Fig. 4 *D–F*; no significant difference, $P = 0.82$, two-way ANOVA; data from five cells/four control mice and seven cells/four KO mice), suggesting that the basal *P*r is not affected in mutant animals.

***P*r Measured with Unitary Synaptic Currents During Trains of High-Frequency Presynaptic Stimulation.** CA3 α-CaMKII-deficient synapses display enhanced frequency facilitation (Fig. 3 *D–F* and *I*) but unchanged basal *P*r (Fig. 4 *A–F*). This suggests that the activity-dependent increase in *P*r, which occurs when synapses are stimulated with high frequency (30), is enhanced in mutant mice. To obtain a direct estimate of *P*r during high-frequency presynaptic stimulation, we recorded short trains (consisting of 15 stimuli, delivered with 50-ms interpulse interval) of unitary EPSCs in slices from control and CA3 α-CaMKII KO mice. Unitary synaptic responses in the CA1 neuron were evoked by low-intensity stimulation of a presynaptic CA3 cell body (22). Two different selection criteria were applied to identify true unitary responses in the CA3-CA1 cell pairs that were subsequently used for further analysis. First, a sharp all-or-none threshold of stimulation intensity for the appearance of EPSCs in response to the focal presynaptic stimulation was taken as evidence of the unitary nature of the

synaptic responses (22) (Fig. 4*G*). Second, to confirm that the EPSCs recorded under these conditions are unitary, we tested the effects of paired-pulse stimulation (50-ms interpulse interval) on synapses that passed the intensity threshold test. Only the cell pairs that did not show any change in the mean size of the actual responses, not including failures of synaptic transmission (potency) (23), during paired-pulse stimulation (26) (Fig. 4*H*) were used for *P*r measurements during the above-mentioned trains of high frequency presynaptic stimulation. Under these conditions, minimal stimulation recruits a single release site, and the potency is equivalent to quantal size (23). When these unitary synapses were repeatedly stimulated, we found that, although *P*r was virtually identical in control and CA3 α-CaMKII-deficient synapses during the initial part of the stimulation train, it was significantly enhanced in the mutant synapses in response to the subsequent stimuli (Fig. 4 *I* and *J*; data from eight cells/six control mice and from five cells/five KO mice; significant difference, F[1,11] = 10.92; *P* < 0.01, two-way ANOVA).

Discussion

These results provide the first direct evidence, to our knowledge, that α-CaMKII serves an essential function in neurotransmitter release by placing an inhibitory constraint on release during high-frequency presynaptic activity. How does α-CaMKII exert its function in *P*r regulation? α-CaMKII has numerous presynaptically localized substrates that are known to be involved in neurotransmitter release (2). One recent study has shown that abolishing the expression of the synaptic vesicle protein Rab3A, which interacts with the CaMKII substrate rabphilin, and its putative effector in regulating synaptic vesicle fusion, the active zone protein RIM1α, was accompanied by an enhancement in frequency facilitation similar to that seen at CA3 α-CaMKII-deficient synapses (34). However, synapses lacking RIM1α or Rab3A also showed an increase in PPF, indicating a change in the baseline *P*r in these mutant mice. This is in contrast with our study in which PPF in CA3 α-CaMKII KO mice was not affected, suggesting the CA3 α-CaMKII KO phenotype may involve different molecular targets. Such a target could be the CaMKII substrate, the N-type Ca^{2+} channel, which is located at presynaptic terminals and mediates evoked neurotransmitter release (1). Phosphorylation of the synaptic protein interaction site (synprint site) on the N-type calcium channel inhibits its interaction with SNARE proteins, literally disconnecting N-type Ca-channels from syntaxin1A and SNAP-25 (35) and essentially moving synaptic vesicles further from the calcium influx. This mechanism may lead to a CaMKII-dependent decrease in *P*r and could provide a way to decrease neurotrans-

mitter release during high-frequency presynaptic stimulation, because CaMKII decodes the frequency of Ca^{2+} spikes into distinct amounts of kinase activity (36). This negative regulation would be lifted in CA3 α-CaMKII-deficient synapses. Such a regulatory mechanism could maintain wild-type synapses in an optimal range of release probabilities necessary for normal synaptic operation (1, 30), because efficient neuronal computation requires that *P*r retain a large dynamic range (37). In addition, α-CaMKII may also affect cytoskeletal proteins and calcium homeostasis in general (3, 6), which could lead to changes in release process.

What is the potential physiological significance of the observed phenotype? One possibility is that CaMKII-dependent regulation of *P*r might be involved in the modulation of oscillatory activity in the hippocampus. A prominent feature of neuronal networks in different mammalian brain regions, including the hippocampus, is the presence of oscillations at different frequencies (38, 39). Oscillating pyramidal cells generate periodic bursts of action potentials in a synchronized manner across the neuronal network (40, 41). Recent experiments have shown that the duration of the high-frequency CA3 burst is limited by depression of the excitatory recurrent collateral synapses in the CA3 network, which is mediated by a decrease in glutamate release (42). It has been demonstrated that the interval between bursts critically depends on the rate of recovery of releasable vesicles and the *P*r at these synapses (42). Such bursts may provide the most efficient stimulus for exciting the cells that receive synaptic input from the firing neurons (43), and therefore, the presynaptic factors capable of controlling the probability of occurrence and duration of the burst may have serious implications for information processing. Our findings suggest a possible role for CaMKII in the regulation of the probability and duration of synchronous discharges of the CA3 neuronal network (43, 44) and propagation of the CA3 oscillations to the CA1 area. Such a regulatory mechanism could be involved in the shaping of the oscillatory behavior in the hippocampus, which has been implicated in hippocampal memory processing (40).

1. Cowan, W. M., Sudhof, T. C. & Stevens, C. F., eds. (2001) *Synapses* (Johns Hopkins Univ. Press, Baltimore).
2. Fernandez-Chacon, R. & Sudhof, T. C. (1999) *Annu. Rev. Physiol.* **61**, 753–776.
3. Lisman, J., Schulman, H. & Cline, H. (2002) *Nat. Rev. Neurosci.* **3**, 175–190.
4. Malinow, R., Schulman, H. & Tsien, R. W. (1989) *Science* **245**, 862–866.
5. Silva, A. J., Stevens, C. F., Tonegawa, S. & Wang, Y. (1992) *Science* **257**, 201–206.
6. Braun, A. P. & Schulman, H. (1995) *Annu. Rev. Physiol.* **57**, 417–445.
7. Mayford, M., Wang, J., Kandel, E. R. & O'Dell, T. J. (1995) *Cell* **81**, 891–904.
8. Giese, K. P., Fedorov, N. B., Filipkowski, R. K. & Silva, A. J. (1998) *Science* **279**, 870–873.
9. Hinds, H. L., Tonegawa, S. & Malinow, R. (1998) *Learn. Mem.* **5**, 344–354.
10. Margrie, T. W., Rostas, J. A. & Sah, P. (1998) *Nat. Neurosci.* **1**, 378–383.
11. Wu, G., Malinow, R. & Cline, H. T. (1996) *Science* **274**, 972–976.
12. Griffith, L. C., Verselis, L. M., Aitken, K. M., Kyriacou, C. P., Danho, W. & Greenspan R. J. (1993) *Neuron* **10**, 501–509.
13. Shirke, A. M. & Malinow, R. (1997) *J. Neurophysiol.* **78**, 2682–2692.
14. Llinas, R., McGuinness, T. L., Leonard, C. S., Sugimori, M. & Greengard P. (1985) *Proc. Natl. Acad. Sci. USA* **82**, 3035–3039.
15. Llinas, R., Gruner, J. A., Sugimori, M., McGuinness, T. L. & Greengard, P. (1991) *J. Physiol.* **436**, 257–282.
16. Rosahl, T. W., Geppert, M., Spillane, D., Herz, J., Hammer, R. E., Malenka, R. C. & Sudhof, T. C. (1994) *Cell* **75**, 661–670.
17. Chapman, P. F., Frenguelli, B. G., Smith, A., Chen, C. M. & Silva, A. J. (1995) *Neuron* **14**, 591–597.
18. Lin, R. C., Kapiloff, M. S., Durgerian, S., Tatemoto, K., Russo, A. F., Hanson, P., Schulman, H. & Rosenfeld, M. G. (1987) *Proc. Natl. Acad. Sci. USA* **84**, 5962–5966.
19. Buchholz, F., Angrand, P. O. & Stewart, A. F. (1998) *Nat. Biotechnol.* **16**, 657–662.
20. Zeng, H., Chattarji, S., Barbarosie, M., Rondi-Reig, L., Philpot, B. D., Miyakawa, T., Bear, M. F. & Tonegawa, S. (2001) *Cell* **107**, 617–629.
21. Nakazawa, K., Quirk, M. C., Chitwood, R. A., Watanabe, M., Yeckel, M. F., Sun, L. D., Kato, A., Carr, C. A., Johnston, D., Wilson, M. A. & Tonegawa, S. (2002) *Science* **297**, 211–218.
22. Bolshakov, V. Y., Golan, H., Kandel, E. R. & Siegelbaum, S. A. (1997) *Neuron* **19**, 635–651.
23. Stevens, C. F. & Wang, Y. (1994) *Nature* **371**, 704–707.
24. Hamilton, D. L. & Abremski, K. (1981) *J. Mol. Biol.* **178**, 481–486.
25. Kontgen, F., Suss, G., Stewart, C., Steinmetz, M. & Bluethmann, H. (1993) *Int. Immunol.* **5**, 957–964.
26. Dobrunz, L. E. & Stevens, C. F. (1997) *Neuron* **18**, 995–1008.
27. Stevens, C. F. & Wang, Y. (1995) *Neuron* **14**, 795–802.
28. Dittman, J. S., Kreitzer, A. C. & Regehr, W. G. (2000) *J. Neurosci.* **20**, 1374–1385.
29. Wu, L. G. & Borst, J. G. (1999) *Neuron* **23**, 821–832.
30. Zucker, R. S. & Regehr, W. G. (2002) *Annu. Rev. Physiol.* **64**, 355–405.
31. Huang, E. P. & Stevens, C. F. (1997) *J. Neurophysiol.* **78**, 2870–2880.
32. Hessler, N. A., Shirke, A. M. & Malinow, R. (1993) *Nature* **366**, 569–572.
33. Rosenmund, C., Clements, J. D. & Westbrook, G. L. (1993) *Science* **262**, 754–757.
34. Schoch, S., Castillo, P. E., Jo, T., Mukherjee, K., Geppert, M., Wang, Y., Schmitz, F., Malenka, R. C. & Sudhof, T. C. (2002) *Nature* **415**, 321–326.
35. Yokoyama, C. T., Sheng, Z. H. & Catterall, W. A. (1997) *J. Neurosci.* **17**, 6929–6938.
36. Koninck, P. D. & Schulman, H. (1998) *Science* **279**, 227–230.
37. Zador, A. (1998) *J. Neurophysiol.* **79**, 1219–1229.
38. Buzsaki, G. (2002) *Neuron* **33**, 325–340.
39. Whittington, M. A., Traub, R. D., Faulkner, H. J., Stanford, I. M. & Jefferys, J. G. (1997) *Proc. Natl. Acad. Sci. USA.* **94**, 12198–12203.
40. Fisahn, A., Pike, F. G., Buhl, E. H. & Paulsen, O. (1998) *Nature* **394**, 186–189.
41. Staley, K. J., Bains, J. S., Yee, A., Hellier, J. & Longacher, J. M. (2001) *J. Neurophysiol.* **86**, 2736–2747.
42. Staley, K. J., Longacher, M., Bains, J. S. & Yee, A. (1998) *Nat. Neurosci.* **1**, 201–209.
43. Lisman, J. E. (1997) *Trends Neurosci.* **20**, 38–43.
44. Bains, J. S., Longacher, J. M. & Staley, K. J. (1999) *Nat. Neurosci.* **2**, 720–726.

Hinds *et al.*